

Research Journal of Pharmaceutical, Biological and Chemical Sciences

Preliminary Evaluation of Technetium-99m-Labeled Thymoquinone: Radiotracer Uptake Studies using Gamma Scintigraphy Imaging Technique.

Reelma Velho-Pereira¹, Aart Jagtap¹, Rajiv V. Gaikwad², and Jomana Elaridi^{3*}.

¹Department of Pharmacology, Bombay College of Pharmacy, Mumbai University, Mumbai-400 098, India.

²Department of Veterinary Nuclear Medicine, Bombay Veterinary College, Parel Mumbai 400 012, India.

³Department of Natural Sciences, Lebanese American University, P.O. Box 13-5053, Chouran Beirut 1102 2801, Lebanon.

ABSTRACT

Thymoquinone (TQ) was radiolabeled with sodium pertechnetate ($\text{Na}^{99\text{m}}\text{TcO}_4$) by reduction with stannous chloride (SnCl_2). The labeling efficiency of $^{99\text{m}}\text{Tc}$ -TQ was determined by iTLC. Labeling conditions were optimized for pH, amount of SnCl_2 required for radiolabeling and incubation time. Specifically, direct radiolabeling of 2.5 mg/ml TQ with 250 $\mu\text{g}/\text{ml}$ of stannous chloride at pH 7 with gentle mixing and incubation for 30 minutes generated the desired $^{99\text{m}}\text{Tc}$ -TQ complex with 95% labeling efficiency. The *in vitro* stability in serum and physiologic saline showed that the radiolabeled complex was stable for 24 h. Based on the percent injected dose (%ID), the highest uptake of the $^{99\text{m}}\text{Tc}$ -TQ was found in the RES post IV injection in normal mice. Oral administration of TQ led to predominant uptake of the radiolabeled complex in the stomach and the intestine. Thus, a quick, efficient and reproducible method for radiolabeling thymoquinone with the $^{99\text{m}}\text{Tc}$ -radionuclide was developed and optimized. The TQ-radiotracer was evaluated for radiochemical purity, stability and tissue and organ distribution in mice.

Keywords: thymoquinone, radiolabeling, technetium-99m, biodistribution, gamma scintigraphy, radiotracer.

**Corresponding author*

INTRODUCTION

Black seed (*Nigella sativa* Linn) has been used for thousands of years in many Asian and Middle Eastern countries as a protective health remedy in traditional medicine [1-5]. Thymoquinone (TQ) (**Figure 1**) is the main active constituent of the black seed extract and has been reported to have chemopreventive and therapeutic properties, in addition to antihypertensive, antimicrobial, antioxidant, anti-inflammatory and antineoplastic effects [6-8]. TQ has been reported to exhibit antitumor activities, including anti-proliferative and pro-apoptotic effects on cell lines derived from breast, colon, ovary, larynx, lung, myeloblastic leukemia and osteosarcoma [9-12]. Reports have indicated that the growth inhibitory effects of TQ are specific to cancer cells and it is minimally toxic to non-neoplastic cells [12-15]. This has been observed in prostate cancer, colon cancer, canine osteosarcoma, and skin cancer. Many multidrug-resistant variants of human pancreatic adenocarcinoma, uterine sarcoma, and leukemia were found to be sensitive to TQ.^[16] The effectiveness of TQ as an antitumor agent has also been documented in animal experiments [5,17].

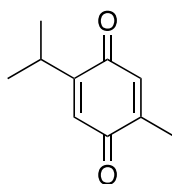


Fig. 1 Structure of thymoquinone

Despite its promising anti-cancer effects, thymoquinone (TQ) has not made significant strides to the clinical level. This may be attributed to its lipophilicity which is associated with poor bioavailability and potentiates problems for oral as well as parenteral delivery. In addition, lack of pharmacodynamic and pharmacokinetic data precludes advancement of TQ into clinical trials. Some of these limitations may be overcome by labeling thymoquinone (TQ) with a radioactive isotope and then following its metabolic route by means of radiodetection [18].

Gamma scintigraphy (γ -scintigraphy) is a widely used radionuclide imaging technique that involves radiolabeling a drug with a γ -emitting radionuclide, such as technetium-99m (^{99m}Tc) [19,20]. Technetium-99m is the most widely used radionuclide in clinical nuclear medicine as it possesses both chemical and physical characteristics which make it the workhorse of radionuclide imaging [21]. Technetium-tagged compounds have technetium bound to a localizing moiety (transporter/drug) that transports technetium to a specific site in the body determined by the properties of the transporter/drug. The main advantage of using a gamma-emitting radionuclide is that it permits a non-invasive whole-body scintigraphic imaging technique for monitoring the biodistribution of a radiolabeled drug in small animals for extended periods of time. This eliminates the need to sacrifice animals at several time points post injection to quantify the disposition profile in time. In addition, dynamic scans can be recorded to monitor the pharmacokinetic behavior on second- or minute-based intervals. Preclinically, this technique is a valuable tool in addition to the so called 'ex vivo' studies comprising the dissection of tissue and subsequent counting of radioactivity.

In the present study, a radiotracer scintigraphic method was developed for studying the *in vivo* biodistribution of TQ in mice using technetium-99m (^{99m}Tc) as a radionuclide.

MATERIALS AND METHODS

TQ was purchased from Sigma–Aldrich Chemicals Pvt. Ltd. (St. Louis, MO, USA). All other chemicals, reagents and solvents were of analytical grade and purchased from Merck India Ltd. (Mumbai, India) and SD Fine-Chemicals Ltd. (Mumbai, India). Sodium pertechnetate ($\text{Na}^{99m}\text{TcO}_4$), separated from molybdenum-99 by solvent extraction method, was procured from BRIT, Mumbai.

Instrumentation:

The Veterinary Nuclear Medicine Center (VNMC) is equipped with Millennium MPS Acquisition System. The Millennium MPS system has a square detector fitted to a floor-mounted gantry and fitted with a

Low Energy General Purpose (LEGP) collimator manufactured by G.E. (General Electric). The acquisition of images (dynamic and static) was performed by using GENIE acquisition station and transferred to eNTEGRA workstation for further processing. The eNTEGRA workstation is equipped with statistical programs to process image / curves suitable for the assessment of function/radionuclide distribution in an interest organ.

Experimental

Radiosynthesis of TQ:

TQ was radiolabeled with $\text{Na}^{99\text{m}}\text{TcO}_4$ by reduction with stannous chloride similar to the reported methods [22]. Briefly, in a sterile vial the pertechnetate (4 mCi) was reduced with 250 μg of stannous chloride dihydrate in 25 μl of freshly prepared 0.1 N HCl and pH was adjusted to 5.5 - 6 with 0.1 M sodium bicarbonate solution. To this, 125 μl of TQ stock solution was added and the solution was allowed to mix in a sonicator at room temperature for 30 minutes. The contents were passed through 0.22 μ filter into an evacuated sterile sealed vial and volume made up with 0.1 M sterile tris buffer to 1 ml (final pH = 7).

Quality control of $^{99\text{m}}\text{Tc-TQ}$:

The labeling efficiency of $^{99\text{m}}\text{Tc-TQ}$ was determined by ascending instant thin layer chromatography (ITLC) using silica gel-coated sheets. The radioactive contaminants were identified as reduced/hydrolyzed (R/H)- $^{99\text{m}}\text{technetium}$ and free $^{99\text{m}}\text{Tc-pertechnetate}$. The thin layer chromatography (TLC) strip (1x10 cm) was spotted with 2 μl of the $^{99\text{m}}\text{Tc}$ -labeled TQ and developed using acetone as the mobile phase. After the solvent front reached the end point (9 cm from the origin), the strip was removed and was cut a 1/3rd from the bottom and 2/3rd from the top. The radioactivity in each strip was determined by a well-type gamma ray spectrophotometer. The free $^{99\text{m}}\text{Tc-pertechnetate}$ migrates to the top portion of the TLC strip ($R_f = 0.9-1.0$), leaving the R/H- $^{99\text{m}}\text{Tc}$ along with the labeled complex ($^{99\text{m}}\text{Tc-TQ}$) at the bottom ($R_f = 0$). Incorporation of excess stannous chloride for reduction of pertechnetate leads to the formation of undesirable radiocolloids. Radiocolloid formation was determined by using a pyridine:acetic acid:water (3:5:1.5) mixture as the mobile phase. The radiocolloids remained at the bottom of the strip, while both the free $^{99\text{m}}\text{Tc-pertechnetate}$ and $^{99\text{m}}\text{Tc-TQ}$ migrated with the solvent front. By subtracting the migrated activity with the solvent front of acetone from that using pyridine:acetic acid:water mixture, the net amount of $^{99\text{m}}\text{Tc-TQ}$ was calculated. The use of two solvent systems proved to be a very accurate method in clearly distinguishing and quantifying the relative amounts of free $^{99\text{m}}\text{Tc}$, R/H $^{99\text{m}}\text{Tc}$, and $^{99\text{m}}\text{Tc-TQ}$.

Optimization of Labeling Conditions:

The radiolabeling procedure was conducted under conditions of various concentrations of stannous chloride, pH, and incubation time to determine conditions for optimal labeling efficiency. Specifically, TQ was radiolabeled using 25, 50, 75, 100, 150 and 250 $\mu\text{g/ml}$ of stannous chloride. The effect of pH was then studied by labeling TQ at pH 5, 5.5, 6.0, 6.5, 7.0 and 7.5. Lastly, incubation times of 5, 10, 15, 20, 25 and 30 minutes were assessed. All experiments were conducted in triplicate ($n = 3$) and the mean values of labeling efficiency are presented. Radiolabeling efficiency was determined using ascending instant thin layer chromatography as previously described.

In vitro stability of $^{99\text{m}}\text{Tc-TQ}$ in saline and in plasma:

The optimized radiolabeled complex was assessed for stability *in vitro* in saline and in plasma by ascending iTLC technique. The labeled complex (0.1 ml) was incubated with freshly collected human plasma and/or saline (0.4 ml) at 37°C for up to 24 h. The samples were withdrawn at 4, 8, 12, 26 and 24 h and analyzed in the dose calibrator. Aliquots at different time intervals were applied on a TLC strip using the procedure previously described. All experiments were conducted in triplicate ($n = 3$).

In vivo Study:

Swiss female albino mice weighing 25-30 g were purchased from Haffkines, Parel. The animals were housed in standard polypropylene cages with wire mesh top and maintained at $23 \pm 2^\circ\text{C}$ and relative humidity $60 \pm 5\%$ with 12 h light-dark cycle, at Bombay Veterinary College (BVC), Parel. Animals were fed a commercially available standard rodent pellet diet (Amrut rat and mice feed manufactured by Nav Maharashtra Chakan Oil

mill Limited, Pune). Water was provided to the animals *ad libitum*. Animal experimentation protocols were approved by the Institutional Animal Ethics Committee of BVC, Mumbai. All studies were performed in accordance with the guidelines of the Committee for the Purpose of Control and Supervision on Experiments on Animals (CPCSEA).

Gamma scintigraphy was used to acquire a better understanding of the whole body localization of a therapeutic dose of ^{99m}Tc -TQ.

For IV administration: Mice (n = 6) were fasted overnight before experiment, but were allowed access to water *ad libitum*. Prior to the start of the experiment, the mice were anaesthetized with a combination of ketamine and xylazine administered intraperitoneally wherein xylazine (10 mg/kg body weight) was used as preanaesthetic agent and ketamine (100 mg/kg body weight) was employed as anesthetic agent. For *in vivo* studies, ^{99m}Tc -TQ complex was administered intravenously at 10 mg/kg body weight as a single dose. The mice were placed in a ventral (sternal) recumbent position with head extended forward under the Millenium MPS single head Gamma camera (GE) fitted with LEGP pin hole collimator and images were acquired by using GENIE acquisition station. Dynamic images were acquired for 30 minutes while the static images were acquired for 1 minute at hourly intervals, for 24 h post injection. The dynamic images were acquired in 64 x 64 matrix for 30 minutes (frame/0.25 sec for 2 minutes followed by frame/10sec for 28 minutes), whereas the static images were acquired in 256 x 256 matrix at 140 keV and 20% window for 1 minute at hourly intervals, for 24 h post injection. The images acquired were transferred to eNTEGRA workstation for further processing. The scintigrams obtained were analyzed by drawing region of interests (ROIs) on the dynamic and static images. Time activity curves (TAC) for 30 minutes were obtained from the dynamic images for the organs of interest like the liver, lung, heart, kidney and bladder. In addition, to validate the results obtained from the static images, the mice were sacrificed at various time points and the organs were dissected and the percentage uptake of the radiolabeled complex was calculated as %ID per g of tissue/organ. Blood was obtained by cardiac puncture at predetermined time points. Subsequently, tissues (heart, lung, liver, spleen, kidney, stomach, intestine), were dissected, washed with normal saline, made free from adhering tissues and dried in the paper folds. The organs were then weighed on an analytical balance and the radioactivity in each organ was measured using a dose calibrator and results expressed as percent injected dose per gram/tissue after decay correction *i.e.* the activity in each organ was divided by the total activity administered to determine the percentage of radioactivity (%ID) in each organ. The %ID was divided by the mass of each tissue to determine the percentage of radioactivity per gram (%ID/g) after applying the decay correction. All data are reported as mean \pm SD. The analysis of images was done by drawing a constant region of interest (ROI) as shown in **Figure 2**. ROIs were drawn on the heart, liver, urinary bladder and time activity curves were plotted. For analysis of static images, a constant region of interest (ROI) was drawn on the heart, liver, urinary bladder and the %ID vs time was plotted.

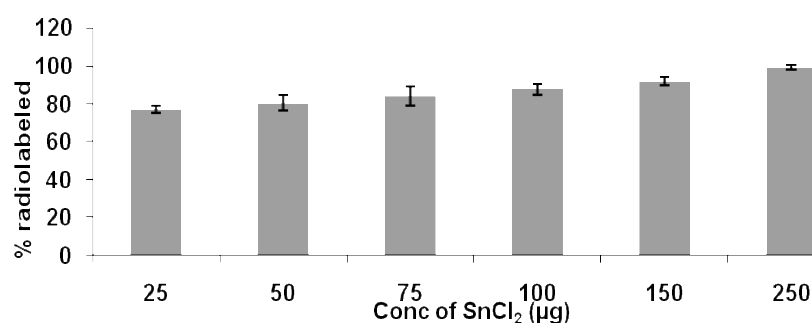


Fig. 2 Effect of amount of stannous chloride on the labeling efficiency of ^{99m}Tc -TQ

For oral administration: The same procedure was followed for oral administration with a slight modification in the anesthesia procedure. Ketamine was administered intraperitoneally (100 mg/kg body weight) prior to oral administration of the radiolabeled complex *via* a feeding needle.

RESULTS AND DISCUSSION

TQ was radiolabeled with ^{99m}Tc by stannous chloride reduction method. The the pertechnetate ($^{99m}\text{TcO}_4^-$) exists in the heptavalent oxidation state and was reduced to lower valence states by stannous

chloride. The labeling efficiency and stability of the labeled complex were ascertained by ascending instant thin layer chromatography (iTLC). The influence of the concentration of stannous chloride on radiolabeling efficiency was evaluated and results are shown in **Figure 3**. The amount of stannous chloride was varied from 25 – 250 µg/ml. Concentrations of stannous chloride less than 50 µg/ml led to poor labeling efficiency (<80%) and greater amounts of free ^{99m}Tc were observed. On the other hand, higher concentrations of stannous chloride (> 250 µg/ml) led to the formation of the undesirable R/H ^{99m}Tc colloid. An optimal ^{99m}Tc-radiolabeling efficiency of 95% was achieved, with traces of radiocolloid (<0.1%), by using 250 µg/ml SnCl₂.2H₂O.

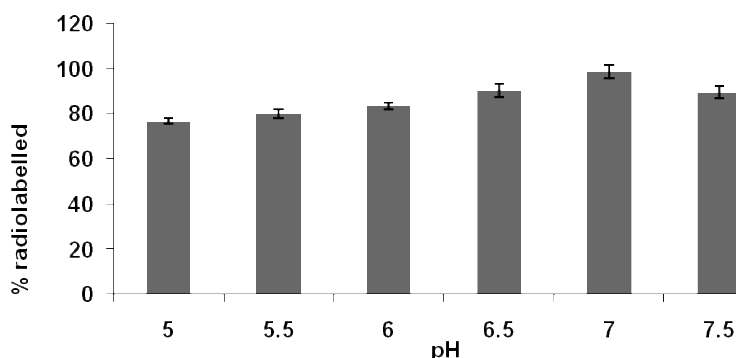


Fig. 3 Effect of pH on the labeling efficiency of ^{99m}Tc-TQ

Thymoquinone was radiolabeled with ^{99m}Tc at various pH values from 5 – 7.5 to assess the effect of pH on radiolabeling efficiency (**Figure 4**). Optimal radiolabeling efficiency (95%) was observed at pH 7.0. Radiocolloid formation was circumvented at neutral pH. Radiolabeling under acidic conditions decreased labeling efficiency, which may be due to precipitation of radiolabeled and free TQ from the solution. The incubation time for the reaction mixture was varied from 5 - 30 minutes as shown in **Figure 5**. Incubation time of 30 minutes resulted in the highest labeling efficiency.

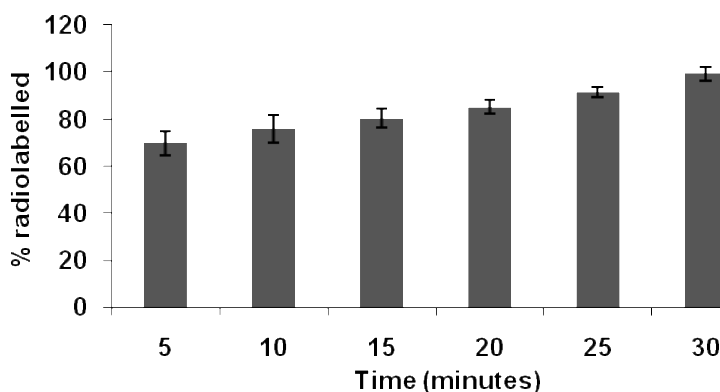


Fig. 4 Effect of incubation time on the labeling efficiency of ^{99m}Tc-TQ

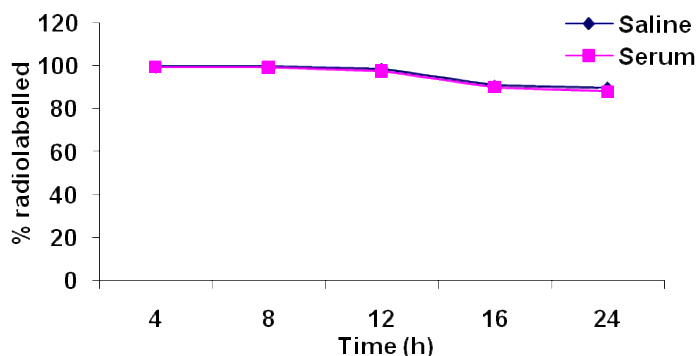


Fig. 5 Stability of the radiolabeled complex ^{99m}Tc-TQ in serum and in saline

Thus, optimal conditions for ^{99m}Tc-TQ radiosynthesis involved the incubation of 2.5 mg/ml TQ, 250 µg/ml of SnCl₂.2H₂O at pH 7.0 for 30 minutes. These conditions produced the desired ^{99m}Tc-TQ radiotracer with 95% labeling efficiency and less than 0.1% of radiocolloid byproducts.

The radiolabeled ^{99m}Tc-TQ conjugate was incubated with human plasma and saline at 37°C and its radiochemical purity was measured at 4, 8, 12, 26 and 24 h. The radiochemical purity of ^{99m}Tc-TQ was maintained at 95% after 4 hours but deteriorated gradually thereafter (Figure 6). However, even after 24 h, the percent of radiolabeled complex in saline and in human serum was still an excellent 89.87% and 87.98% respectively, as determined by ascending instant thin layer chromatography.

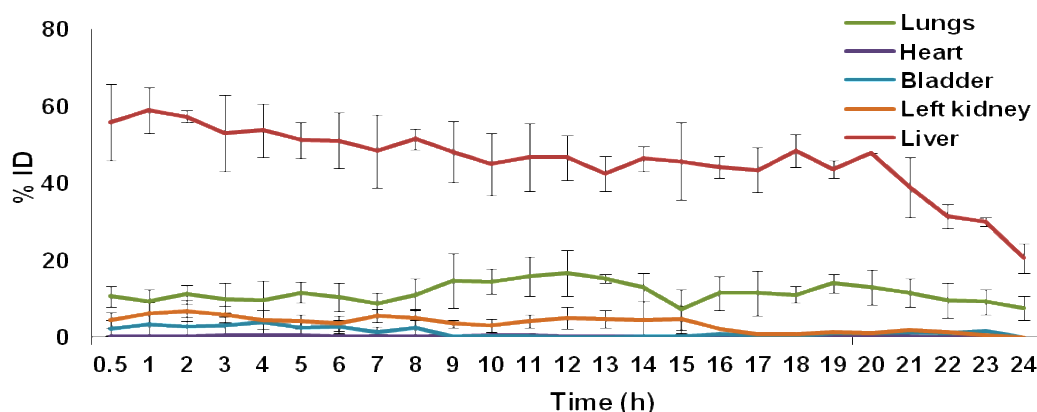


Fig. 6 Distribution of ^{99m}Tc-TQ complex as %ID vs time (h) after IV administration of ^{99m}Tc-TQ in normal mice. Values are obtained after drawing ROIs on the static images for the organs /tissues.

Biodistribution studies were conducted after intravenous and oral administration of the ^{99m}Tc-TQ conjugate and the radiotracer uptake was expressed as percentage of injected dose per tissue of organ (%ID/organ) in mice. The biodistribution of ^{99m}Tc-labeled thymoquinone after 0.5 h, 2 h, 6 h, 8 h, 15 h and 24 h of intravenous injection in mice is shown in Table 1. Based on % injected dose per gram of whole organ, the highest uptake of ^{99m}Tc-TQ was found in the liver, lungs and spleen averaging 18.52, 15.70 and 1.49 respectively, 0.5 h after IV administration of the radiolabeled complex.

Table 1. Biodistribution of ^{99m}Tc-TQ after IV administration in mice based on % ID per gram of whole organ/tissue

Organ/Tissue	0.5 h	2 h	6 h	8 h	15 h	24 h
Heart	0.92 ± 0.02	0.55 ± 0.02	0.22 ± 0.01	0.00 ± 0.01	0.00 ± 0.01	0.00 ± 0.02
Liver	18.52 ± 1.37	28.15 ± 1.24	24.14 ± 1.07	18.68 ± 1.22	13.34 ± 0.96	14.19 ± 1.31
Lung	15.70 ± 2.01	22.26 ± 1.46	19.82 ± 1.40	13.10 ± 2.39	18.77 ± 2.23	18.14 ± 0.54
Spleen	1.49 ± 0.51	3.66 ± 0.04	4.35 ± 0.50	2.36 ± 0.34	2.35 ± 0.38	2.74 ± 0.06
Kidney	1.81 ± 0.04	1.52 ± 0.02	1.23 ± 0.03	1.90 ± 0.05	0.84 ± 0.06	0.93 ± 0.17
Muscle	0.10 ± 0.01	0.07 ± 0.01	0.00 ± 0.00	0.00 ± 0.00	0.00 ± 0.00	0.28 ± 0.20
Bone	0.17 ± 0.05	0.10 ± 0.02	0.15 ± 0.03	0.00 ± 0.02	0.00 ± 0.02	0.00 ± 0.22
Stomach	0.32 ± 0.38	1.63 ± 0.02	1.15 ± 0.03	1.39 ± 0.02	1.25 ± 0.06	0.00 ± 0.01
Intestine	0.34 ± 0.05	0.49 ± 0.03	2.32 ± 0.07	2.99 ± 0.03	0.90 ± 0.03	0.25 ± 0.07
Brain	0.24 ± 0.02	0.16 ± 0.07	0.14 ± 0.02	0.00 ± 0.00	0.00 ± 0.00	0.00 ± 0.00
Tail	0.75 ± 0.04	0.31 ± 0.03	0.60 ± 0.07	0.13 ± 0.05	0.05 ± 0.03	0.00 ± 0.05
Rest of the body	0.20 ± 0.01	0.18 ± 0.07	0.15 ± 0.01	0.45 ± 0.01	0.30 ± 0.01	0.16 ± 0.02
Blood	0.00 ± 0.00	0.10 ± 0.03	0.00 ± 0.01	0.00 ± 0.01	0.00 ± 0.01	0.00 ± 0.01
U.Bladder	0.15 ± 0.01	1.20 ± 0.01	0.00 ± 0.00	0.00 ± 0.00	0.00 ± 0.00	0.00 ± 0.00

The radioactivity in the liver after 24 h was 14.19% while in the lungs and spleen it was averaging 18.14% and 2.74% respectively. The *in vivo* stability of the complex was evident from the lack of affinity of ^{99m}Tc -TQ for the stomach, which is the target organ for free ^{99m}Tc . The biodistribution data in normal mice after IV administration of ^{99m}Tc -TQ suggests that TQ appears to be metabolized in the organs of the RES (liver, lungs and spleen) and is eliminated by the kidneys. The distribution of the ^{99m}Tc -TQ complex in various organs and tissues is presented in **Figure 7**. These results are also supported by the scintigraphic images that show significant radioactivity in the liver, heart, spleen and kidneys. The dynamic images of the mice obtained for the first 30 minutes after intravenous administration of ^{99m}Tc -TQ showed that the radioactivity was found mainly in the abdominal region. Time activity curves (TAC) of the organs are shown in **Figure 8**. The TAC curves of the heart, liver and bladder display rapid clearance of TQ from the heart and a steady and comparatively slower clearance of TQ from the liver.

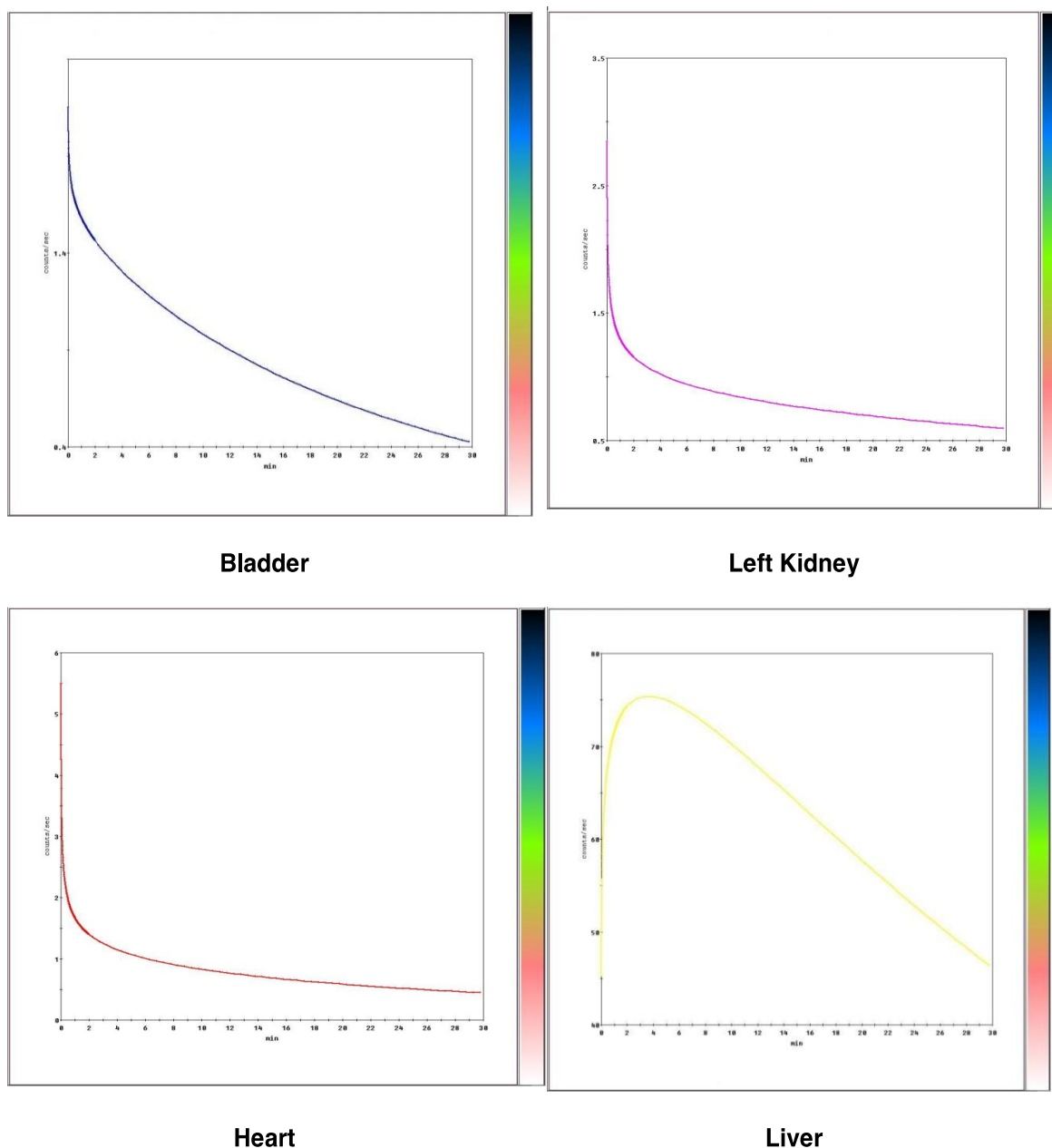


Fig. 7 Time activity curves obtained from the dynamic images of normal mice for the first 30 minutes

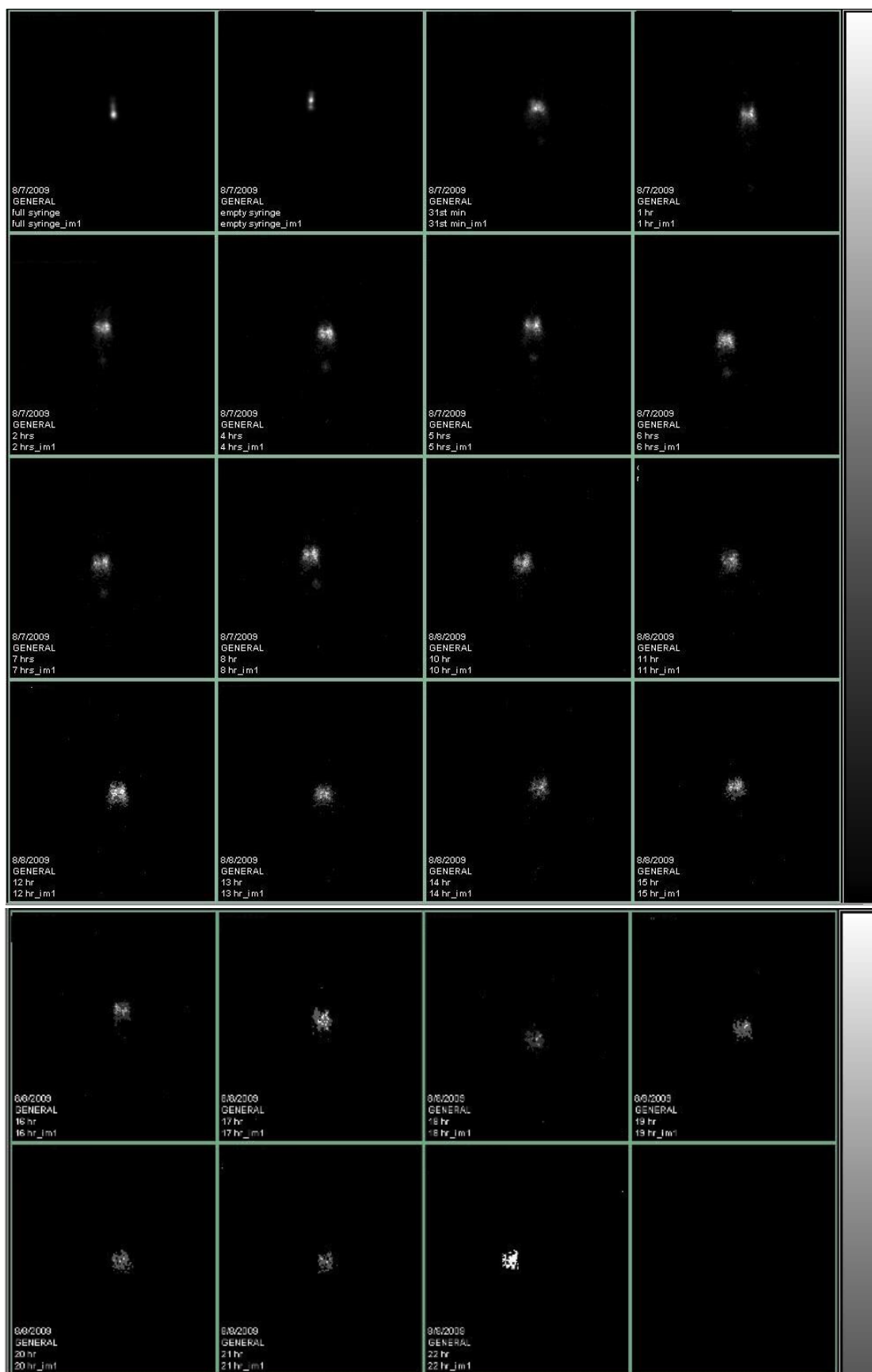


Fig. 8 Static images (1 minute) of mice after IV administration of $^{99m}\text{Tc-TQ}$

Scintigraphic (static) images of mice after intravenous administration of ^{99m}Tc-TQ are shown in **Figure 9** and they complement the results obtained from the biodistribution study. Radioactivity was mainly observed in the abdominal region. The blood pool radioactivity was minimal, as evident by non-visualization of the heart. Radioactivity from the spleen, lung and stomach is partly obscured in the image by the hyper-intense area of the liver.

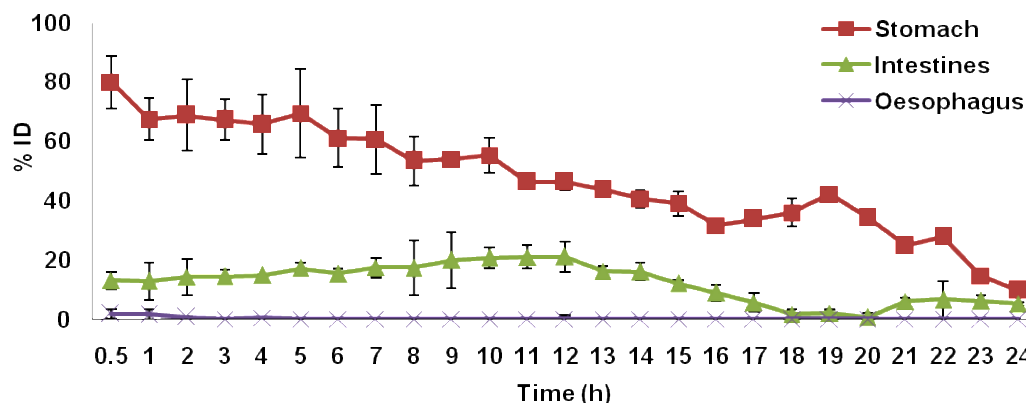


Fig. 9 Distribution of radiolabeled complex as %ID vs time (h) after oral administration of ^{99m}Tc-TQ in normal mice. Values are obtained after drawing ROIs on the static images for the organs /tissues.

Specifically, the static images of mice analyzed by drawing regions of interest (ROIs) on the lungs, liver, bladder, left kidney and liver after IV administration indicated that ^{99m}Tc-TQ had a high uptake by the liver and lungs. Furthermore, the radiolabeled complex was presumably excreted by the kidneys, as there was a steady clearance of the radiolabel from the kidney and bladder. The high percentage of radioactivity recorded in the highly perfuse fenestrated organs, such as the liver and spleen, could be accounted for as the combined activity of the circulating blood passing through the organs as well as due to particle uptake by cells of the RES. The liver demonstrated the greatest accumulation of the radiotracer in terms of %ID. This is expected as the liver is the usual metabolizing organ for most drugs and here it seems more so for TQ.

Biodistribution data on % injected dose per gram of whole organ after oral administration of ^{99m}Tc-TQ at hourly intervals are shown in **Table 2** and presented graphically in **Figure 10**. The highest uptake of the radiolabeled complex was observed to be in the stomach and intestine. The radioactivity in the stomach was reduced considerably from 38.83% at 4 h to 23.63% after 24 h. On the other hand, the radioactivity in the intestine increased significantly from 2.82% at 4 h to 12.80% at 24 h. The rather late appearance of ^{99m}Tc-TQ in the intestine mirrored the high concentrations that still remained in the stomach.

Table 2 Biodistribution of ^{99m}Tc-TQ after oral administration in mice based on % ID per gram of whole organ/tissue

Organ/Tissue	4 h	8 h	18 h	24 h
Heart	2.27 ± 0.02	0.00 ± 0.00	0.00 ± 0.00	0.58 ± 0.01
Liver	0.34 ± 0.01	0.76 ± 0.01	0.00 ± 0.00	0.00 ± 0.00
Lung	0.03 ± 0.00	0.00 ± 0.00	0.00 ± 0.00	0.00 ± 0.00
Spleen	0.00 ± 0.00	0.00 ± 0.00	0.10 ± 0.01	0.00 ± 0.00
Kidney	0.00 ± 0.00	0.00 ± 0.00	0.15 ± 0.01	0.00 ± 0.00
Muscle	0.12 ± 0.01	0.00 ± 0.00	0.00 ± 0.00	0.00 ± 0.00
Bone	0.00 ± 0.00	0.00 ± 0.00	0.00 ± 0.00	0.00 ± 0.00
Stomach	38.83 ± 2.20	48.26 ± 2.35	47.64 ± 4.31	23.63 ± 4.85
Intestine	2.82 ± 1.22	11.95 ± 0.56	11.86 ± 0.17	12.80 ± 0.02
Brain	0.00 ± 0.00	0.00 ± 0.00	0.00 ± 0.00	0.00 ± 0.00

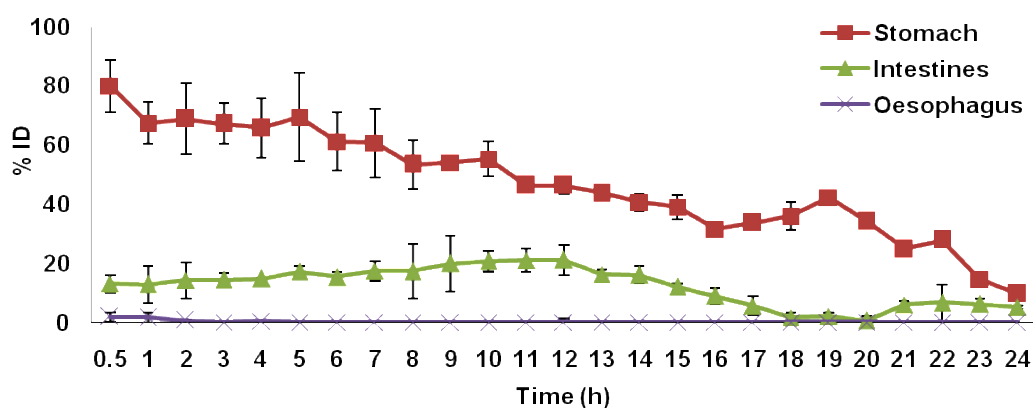
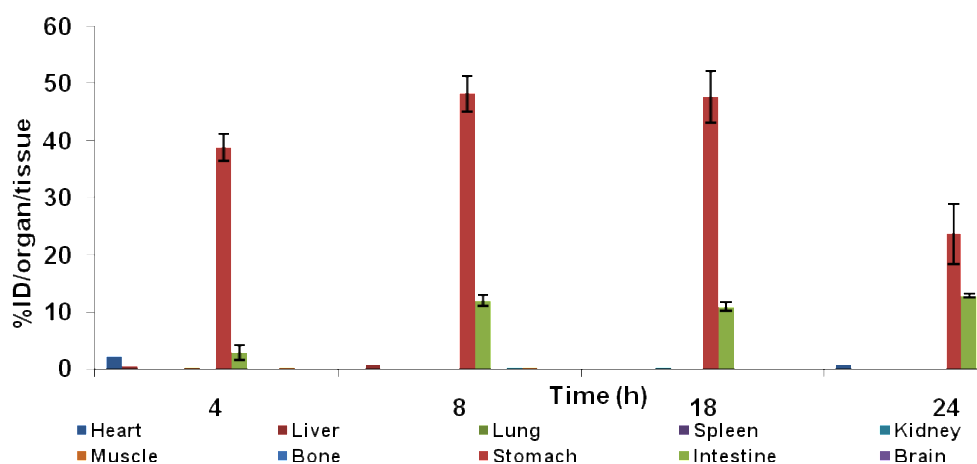


Fig. 10: Distribution of radiolabeled complex in a) various tissues/organs of normal mice at 4, 8, 18 and 24 h after oral administration of ^{99m}Tc-TQ; b) %ID vs time (h) after oral administration of ^{99m}Tc-TQ in normal mice.

Qualitative data obtained by gamma scintigraphy provided additional validation of our biodistribution study. Scintigraphic images of normal mice were analyzed by drawing regions of interest (ROIs) on the stomach, oesophagus and intestine after oral administration of the radiolabeled complex. Evidently, the ^{99m}Tc-TQ radiotracer had maximal accumulation in the stomach and intestine (**Figure 11**). However, radioactivity levels in the stomach and intestine contents decreased considerably with time.

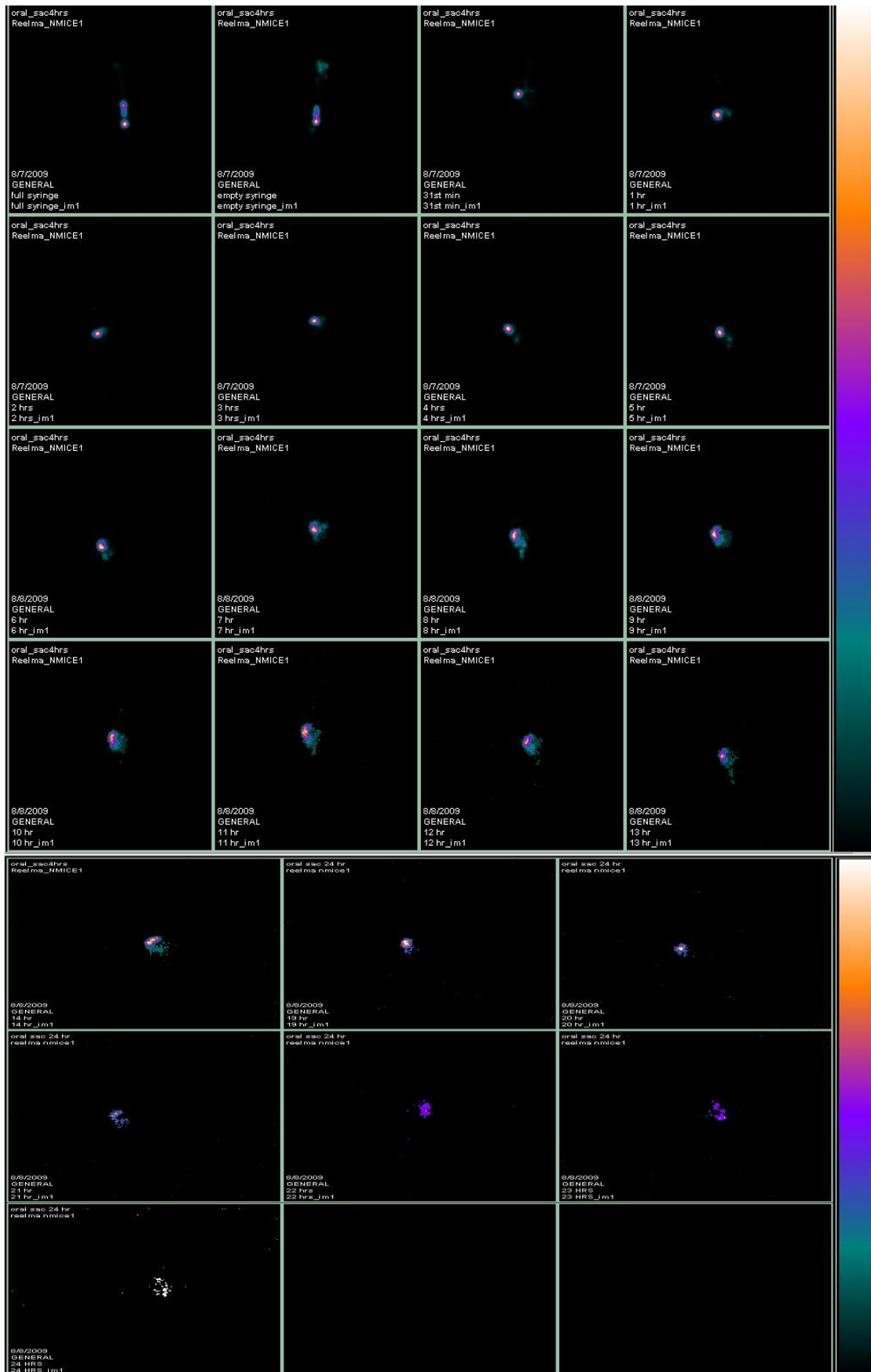


Fig. 11 Static images (1 minute) of mice after oral administration of ^{99m}Tc-TQ.

CONCLUSIONS

Importantly, the biodistribution study and scintigraphic images of the ^{99m}Tc -TQ radiotracer provided quantitative pharmacokinetic data about orally and intravenously administered TQ. This work illustrates the feasibility of radiolabeling TQ and can be applied to evaluate the biodistribution of various formulations of TQ and/or combinative TQ-drug composites in normal and tumor-bearing mice.

ACKNOWLEDGEMENTS

This work was supported by the Dr. Emidio Afonso Memorial Trust and the Indian Pharmaceutical Association – Shri Ramanbhai B. Patel Foundation (IPA-IRF). Dr. Reelma gratefully acknowledges Mr. Mustaque Shaikh for help with computational analysis and Dr. Parag Pawar and Dr. Shalaka for their assistance with scintigraphic studies.

REFERENCES

- [1] Randhawa MA, Alghamdi MS. *Am J Chin Med* 2011; 39: 1075–1091
- [2] Ahmad A, Husain A, Mujeeb M, Khan SA, Najmi A, Siddique NA, Damanhoury ZA, Anwar F. *Asian Pac J Trop Biomed* 2013; 3: 337-352.
- [3] Ali BH, Blunden G. *Phytother Res* 2003; 17: 299-305.
- [4] Deena AS Hussain DAS, and Hussain MM. *Adv Med Plant Res* 2016; 4: 27-57.
- [5] Gali-Muhtasib H, El Najjar N, Schneider-Stock R. The medicinal potential of black seed (*Nigella sativa*) and its components. In: Khan MTH, Ather A, editors. *Lead molecules from natural products: Discovery and new trends*. Elsevier; 2006, pp. 133-153.
- [6] Banerjee S, Padhye S, Azmi A, Wang Z, Philip PA, Kucuk O, Sarkar FH, Mohammad RM. *Nutr Cancer* 2010; 62: 938-946.
- [7] Gali-Muhtasib H, Roessner A, Schneider-Stock R. *Int J Biochem Cell Biol* 2006; 38: 1249-1253.
- [8] El Mezayen R, El Gazzar M, Nicolls MR, Marecki JC, Dreskin SC, Nomiya H. *Immunol Lett* 2006; 106: 72-81.
- [9] Salomi NJ, Nair SC, Panikkar KR. *Nut Cancer* 1991; 16: 67-72.
- [10] Salomi NJ, Nair SC, Jayawardhanan KK, Varghese CD, Panikkar KR. *Cancer Lett* 1992; 31: 41-6.
- [11] Shoieb AM, Elgayyar M, Dudrick PS, Bell JL, Tithof PK. *Int J Oncol* 2003; 22: 107-113.
- [12] Gali-Muhtasib H, Diab-Assaf M, Boltze C, Al-Hmaira J, Hartig R, Roessner A. *Int J Oncol* 2004; 25: 857-866.
- [13] Gali-Muhtasib H, Aboukheir W, Kheir L, Darwiche N, Crooks P. *Anticancer Drugs* 2004; 15: 389-399.
- [14] Worthen DR, Ghosheh OA, Crooks PA. *Anticancer Res* 1998; 18: 1527-1532.
- [15] Kaseb AO, Chinnakannu K, Chen D, Sivanandam A, Tejwani S, Menon M, Dou QP, Reddy GP. *Cancer Res* 2007; 67: 7782-88.
- [16] El-Mahdy MA, Zhu Q, Wang QE, Wani G, Wani AA. *Int J Cancer* 2005; 117: 409-17.
- [17] Mansour MA, Nagi MN, El-Khatib AS, Al-Bekairi AM. *Cell Biochem Funct* 2002; 20: 143-151.
- [18] Lappin G, Temple S. *Radiotracers in Drug Development*. Boca Raton, FL: CRC Press, Taylor & Francis group, 2006.
- [19] Singh AK, Bhardwaj N, Bhatnagar A. *Indian J Pharm Sci* 2004; 66: 18-25.
- [20] Wilding IR, Coupe AJ, Davis SS. *Adv Drug Deliv Rev* 2001; 46: 103-124.
- [21] Saha GB. *Fundamentals of Nuclear Pharmacy*. 6th ed. New York: Springer-Verlag, 2010.
- [22] Harivardhan Reddy L, Sharma RK, Chuttani K, Mishra AK, Murthy RSR. *J Control Release* 2005; 105: 185-198.